Impaired MEK Signaling and SERCA Expression Promote ER Stress and Apoptosis in Insulin-Resistant Macrophages and Are Reversed by Exenatide Treatment

Chien-Ping Liang, Seongah Han, Gang Li, Ira Tabas, and Alan R. Tall

Accumulation of toxic lipids evokes the unfolded protein response (UPR) and apoptotic death of macrophages and vascular cells in atherosclerotic plaques. Primary macrophages from insulin-resistant *ob/ob* and insulin receptor $(Insr)^{-/-}$ mice display increased apoptosis in response to loading with free cholesterol or oxysterol, but underlying mechanisms have not been elucidated. We show increased activation of all three major branches of the UPR in response to free cholesterol or oxysterol loading in insulin-resistant macrophages. Inhibition and rescue experiments revealed that defective MEK/extracellular signal–related kinase (ERK)/cAMP-responsive element–binding protein (CREBP) signaling in insulin-resistant macrophages leads to decreased expression of sarcoplasmic endoplasmic reticulum (ER) Ca^{2+}-ATPase, depletion of ER calcium stores, PKR-like ER kinase activation, and ER stress–associated apoptosis. Activation of macrophage glucagon-like peptide 1 (GLP-1) receptor via the antidiabetic drug exenatide led to improvements in both ERK and AKT signaling and reversed the increase in UPR and apoptosis of insulin-resistant macrophages in atherosclerotic lesions of $ob/ob.Ldlr^{-/-}$ and $Insr^{-/-}.Ldlr^{-/-}$ mice. Increased signaling via GLP-1 receptor or the CREBP activator protein kinase A thus offers a way to rescue insulin-resistant macrophages from excessive ER stress responses and apoptosis in insulin resistance and type 2 diabetes. ***Diabetes*** **61:2609–2620, 2012**

Coronary atherosclerosis and vascular complications are the leading causes of morbidity and mortality in individuals with type 2 diabetes. The mechanisms responsible for increased risk of atherosclerotic disease and complications in type 2 diabetes remain poorly understood (1). Diabetic patients show more advanced atherosclerotic lesions with characteristics of accelerated, lipid-rich necrotic core formation and enhanced macrophage apoptosis in their plaques, apparently predisposing them to plaque rupture, coronary thrombosis, and sudden death (2).

The accumulation of "toxic" lipids in macrophage foam cells in the arterial wall is a central event in the development of atherosclerotic plaques (3). The toxic lipids that accumulate in lesions include unesterified cholesterol, 7-oxysterols, and oxidized phospholipids. The accumulation of these lipids in vascular cells such as macrophages results in apoptotic or necrotic cell death, inciting an inflammatory response that further increases vascular damage (4–7). A variety of different cellular mechanisms are involved in linking toxic lipid accumulation to programmed cell death, such as endoplasmic reticulum (ER) stress, oxidative stress, and changes in organelle permeability. An important mechanism of lipotoxicity involves the ER stress response. Thus, accumulation of saturated fatty acids (8), free cholesterol (9), 7-oxysterols (10), and oxidized phospholipids (5) have all been linked to signals that induce the proapoptotic effects of the ER stress response. Advanced atherosclerotic plaques, especially those associated with atherothrombosis, show evidence of ER stress and apoptosis of macrophages (11), suggesting relevance of in vitro observations to in vivo plaque complications (7). Importantly, deficiency of C/EBP homologous protein (CHOP), a key protein involved in ER stress–induced apoptosis, significantly reduced lesion area, apoptosis, and necrosis in advanced atherosclerosis (12), suggesting that attenuation of the CHOP branch of the unfolded protein response (UPR) could have beneficial effects in this disease. Moreover, oral administration of chemical chaperones, which alleviated aortic ER stress, decreased the formation of atherosclerotic plaques (13,14).

We recently showed that cellular insulin resistance predisposes macrophages to apoptosis induced by loading with free cholesterol or oxidized LDL, contributing to increased macrophage apoptosis and necrotic core formation in advanced atherosclerotic lesions (15). Macrophages from mice genetically deficient in insulin receptors $(Insr^{-/-})$ showed evidence of increased ER stress in the basal state as well as an enhanced ER stress response when challenged with free cholesterol loading (15). Similar to our findings, monocytes from patients with type 2 diabetes, which were known to be resistant to insulin (16), displayed an exaggerated UPR and increased ER stress–induced apoptosis (17). In type 2 diabetes, pancreatic β-cells are also predisposed to ER stress–associated apoptotic cell death (18). However, the mechanisms linking cellular insulin resistance to enhanced cell death when ER stress is induced by various lipotoxic stimuli are not well understood (16).

RESEARCH DESIGN AND METHODS

Animals. Obese *ob/ob*, lean$^{+/+}$, and *ob/+* mice on a C57BL/6J background were obtained from the Jackson Laboratory. Mice deficient in both leptin and Ldlr ($ob/ob;Ldlr^{-/-}$) on a C57BL/6J background were generated as previously described (19). All experiments were performed with animals fed regular rodent chow diet, except in the experiments of in vivo exenatide or saline treatment where $ob/ob;Ldlr^{-/-}$, $Insr^{-/-};Ldlr^{-/-}$, and $Ldlr^{-/-}$ mice were fed a Western-type diet (WTD) (TD88137; Harlan-Teklad). All animal procedures used in this study followed Columbia University's institutional guidelines and relevant regulatory standards.

In vitro treatments and assays of macrophages. Fresh peritoneal macrophages were treated in Dulbecco's modified Eagle's medium (DMEM)/10% FBS with LY294002 (10 μmol/L; Biomol), PD98059 (Calbiochem), U0126 (Sigma-Aldrich),

From the Departments of Medicine, Anatomy and Cell Biology, and Physiology and Cellular Biophysics, Columbia University, New York, New York.
Corresponding author: Chien-Ping Liang, cl534@columbia.edu.
Received 10 October 2011 and accepted 10 April 2012.
DOI: 10.2337/db11-1415
This article contains Supplementary Data online at http://diabetes.diabetesjournals.org/lookup/suppl/doi:10.2337/db11-1415/-/DC1.

rapamycin (2 μmol/L; Calbiochem), GF109203 (2 μmol/L; Sigma-Aldrich), palmitic acid–BSA (0.5 mmol/L; Sigma-Aldrich), thapsigargin (5 μmol/L; Sigma-Aldrich), tunicamycin (2.5 μg/mL; Sigma-Aldrich), 8-Br-cAMP (Sigma-Aldrich), forskolin (Sigma-Aldrich), exendin-4 (California Peptide Research), H-89 (Sigma-Aldrich), Rp-adenosine 3′,5′-cyclic monophosphorothioate (Rp-cAMPS) (Sigma-Aldrich), 6-benzoyl (Bnz)-cAMP (Biolog), 8-pMeOPT-2'-*O*-Me-cAMP (Biolog), or corresponding vehicle controls, acetylated (Ac)LDL (100 μg/mL; Biomedical Technologies) and compound Sandoz 58035 (10 μg/mL; Sigma-Aldrich), oxidized LDL (100 μg/mL; Biomedical Technologies), or 7-ketocholesterol (40 μg/mL; Sigma-Aldrich) for the times specified in figure legends. Mouse macrophages were infected with adenovirus either harboring lacZ (Ad-LacZ) or constitutively active MEK mutant (Ad-MEK), provided by Dr. Shougang Zhuang (Brown Alpert Medical School, Providence, RI), as described previously (20). After treatments, total RNA or cell lysates were prepared for further analysis. Macrophage total RNA isolation and SYBR Green quantitative PCR (QPCR) analysis were performed as previously described (15). Western analysis was performed using the following primary antibodies: anti–phosphorylated eIF2 (P-eIF2) (Cell Signaling), anti-activating transcription factor (ATF)-6 (Imgenex), anti-LaminB1 (Santa Cruz), anti–sarcoplasmic-ER calcium ATPase 2 (SERCA2) (Santa Cruz), anti–phosphorylated cAMP-responsive element–binding protein (P-CREBP) (Upstate Biotechnology), anti-CREBP (Santa Cruz), anti–glucagon-like peptide 1 (GLP-1) receptor (Santa Cruz Biotechnology), anti–phosphorylated PKR-like ER kinase (P-PERK) (Cell Signaling), anti-AKT and phosphorylated AKT (P-AKT) (Cell Signaling), anti-ERK and phosphorylated ERK (P-ERK) (Cell Signaling), anti-MEK (Cell Signaling), anti–ATF-3 (Santa Cruz), and anti–β-actin antibody (Sigma-Aldrich). Apoptosis assays were performed as described previously (15). Macrophage calcium imaging was performed as described previously (21).

Atherosclerotic lesion analysis. Mouse proximal aortas were serially paraffin sectioned as described previously (15). Serial aortic sections were probed with antibody against P-PERK or ATF-3, or control antibody followed by appropriate Alexa Fluor 488–conjugated secondary antibody (Invitrogen) (22). Specific fluorescence signals in the digitized images of proteins colocalized with macrophage marker Mac-3–positive stains were identified using ImageJ (NIH). Lesional macrophage apoptosis was monitored by the transferase-mediated dUTP nick-end labeling (TUNEL) assays and immunohistochemistry with antibody against active caspase-3 (15). TUNEL- or caspase-3–positive signals were determined to colocalize with Mac-3 staining of lesional macrophages.

Statistical analysis. Results were expressed as average ± SE (n is noted in the figure legends or figures), and statistical significance of differences was evaluated with Student t test.

RESULTS

Exaggerated activation of the UPR in response to free cholesterol loading in insulin-resistant macrophages. In this study, we used peritoneal macrophages isolated from either *Insr*$^{-/-}$ or *ob/ob* mice to investigate the mechanisms responsible for an increased UPR in insulin-resistant cells. Three distinct branches of the UPR have been identified involving signaling by PERK, ATF-6, and X-box binding protein 1 (XBP1) (23). To determine whether these were involved in ER stress–induced apoptosis, we monitored the expression of P-eIF2, ATF-6 cleavage, and XBP1 splicing. Basal insulin-resistant macrophages showed an increase in phosphorylation of PERK target eIF2, ATF-6 cleavage, and XBP1 mRNA splicing compared with controls (Fig. 1*A* and *B*). Time-course analysis of the response to free cholesterol loading revealed a more prominent transcriptional induction of UPR-responsive genes *Chop* (PERK branch of UPR) and *Grp78* (an ATF-6 target), and increased Xbp1 splicing in *Insr*$^{-/-}$ cells with a similar time course, suggesting parallel induction of all three major branches of the UPR in insulin-resistant macrophages (Fig. 1*C*). Similar to *Insr*$^{-/-}$ cells (15), freshly isolated macrophages from *ob/ob* mice showed increased PERK phosphorylation and increased apoptosis when challenged with free cholesterol, 7-ketocholesterol, or oxidized LDL loading (Supplementary Fig. 1*A* and *B*). More pronounced expression of some ER stress markers such as CHOP was also found in free cholesterol–loaded *ob/ob* macrophages (Supplementary

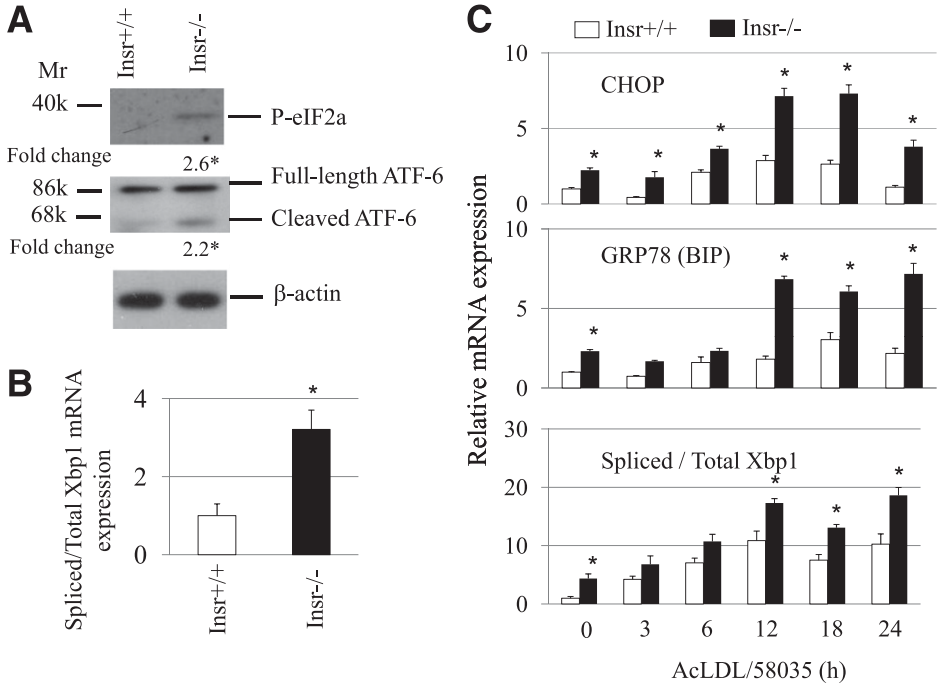

FIG. 1. Insulin-resistant macrophages exhibited elevated UPR. *A*: Fresh peritoneal macrophages from either *Insr*$^{+/+}$ or *Insr*$^{-/-}$ mice fed regular chow diet were cultured at 37°C in DMEM with 10% FBS for 2 h. Cells were harvested and protein extracts were prepared. Western analysis was performed with antibodies against the proteins as indicated. Fold change indicates the expression ratio of *Insr*$^{-/-}$ over *Insr*$^{+/+}$. n = 3. *P < 0.05. *B*: Fresh concanavalin A–elicited peritoneal macrophages isolated from *Insr*$^{+/+}$ and *Insr*$^{-/-}$ mice were cultured as described in *A* and used to determine the levels of total and spliced Xbp1 mRNAs by real-time QPCR. QPCR was performed in triplicate. n = 3. *P < 0.05. *C*: Concanavalin A–elicited macrophages isolated from *Insr*$^{+/+}$ and *Insr*$^{-/-}$ mice were treated with or without AcLDL (100 μg/mL) + compound 58059 (10 μg/mL) for indicated times. The levels of CHOP, 78-kDa glucose–regulated protein (GRP78) (immunoglobulin-binding protein [BIP]), and total and spliced Xbp1 mRNAs were measured by real-time QPCR. QPCR was performed in triplicate. n = 4. *P < 0.05 for *Insr*$^{-/-}$ vs. *Insr*$^{+/+}$ cells at specific time points. Mr, molecular mass; k, kilodalton.

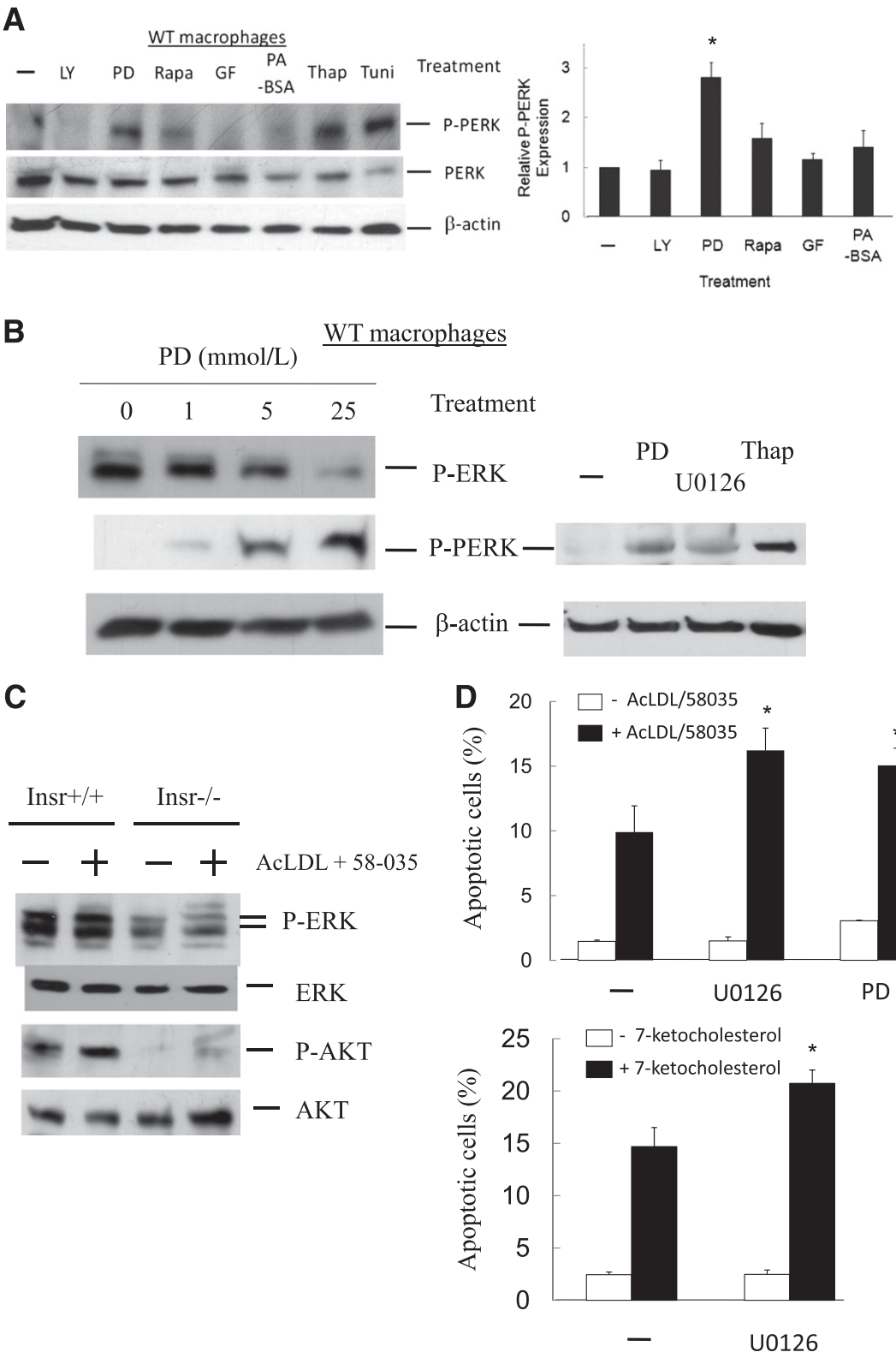

FIG. 2. Inhibition of macrophage MEK signaling induces the UPR and promotes ER stress–associated apoptosis. *A* and *B*: Concanavalin A–elicited peritoneal WT macrophages were treated with inhibitors of PI3K (LY294002 [LY], 10 μmol/L), MEK (PD98059 or U0126, 10 μmol/L), mammalian target of rapamycin (rapamycin [Rapa], 2 μmol/L), protein kinase C (GF109203 [GF], 2 μmol/L), or palmitic acid–BSA (PA-BSA, 0.5 mmol/L) in DMEM with 10% FBS for 12 h. Protein lysate of macrophages treated with thapsigargin (Thap, 5 μmol/L) or tunicamycin (Tuni, 2.5 μg/mL) was used as positive controls. The levels of indicated proteins were determined by Western analysis. Data represent mean ± SEM. $n = 3$. *$P < 0.05$. *C*: Concanavalin A–elicited peritoneal macrophages isolated from *Insr*$^{+/+}$ and *Insr*$^{-/-}$ mice were treated with or without AcLDL (100 μg/mL) + 58-035 (10 μg/mL) for 5 h. The expression of P-ERK, ERK, P-AKT, and AKT was determined by Western analysis. $n = 3$. *D*: WT peritoneal macrophages pretreated with or without the inhibitors of MEK (U0126 or PD98059) were incubated with or without AcLDL (100 μg/mL) and compound 58035 (10 μg/mL) or 7-ketocholesterol (40 μg/mL) at 37°C for ~8 h. Apoptosis of macrophages was determined by annexin V staining. $n = 3$. *$P < 0.05$ for free cholesterol–loaded cells with vs. without the treatment of U0126 or PD98059 compounds. *E* and *F*: Concanavalin A–elicited peritoneal macrophages isolated from *Insr*$^{+/+}$ (WT) and *Insr*$^{-/-}$ mice were infected with adenovirus either harboring lacZ (Ad-LacZ) or constitutively active MEK mutant (Ad-MEK) for ~30 h. Macrophage protein extracts

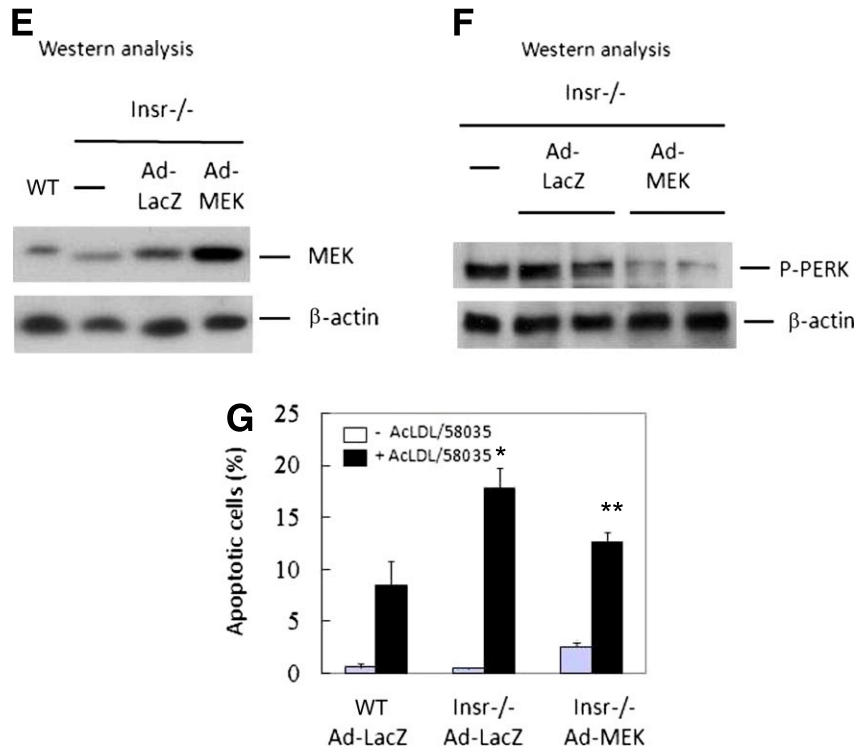

FIG. 2. (*Continued*) were prepared, and Western analysis was performed with antibodies against the proteins as indicated. $n = 3$. *G*: Macrophages pretransduced with adenovirus as described in *E* were incubated with or without AcLDL (100 μg/mL) and compound 58035 (10 μg/mL). Apoptosis was then determined by annexin V staining. $n = 3$. *$P < 0.05$ for free cholesterol–loaded WT vs. $Insr^{-/-}$ cells. **$P < 0.05$ for free cholesterol–loaded $Insr^{-/-}$ cells transduced with Ad-LacZ vs. Ad-MEK.

Fig. 1*C*). An elevation in UPR, however, did not significantly reduce global protein translation (Supplementary Fig. 1*A*, bottom) or increase oxidative stress in *ob*/*ob* versus wild-type (WT) cells, as assessed using reactive oxygen species detection reagents (data not shown).

Impaired macrophage MEK activity downregulates SERCA and induces the UPR. The phosphorylation of PERK is a hallmark of UPR activation and ER stress (23). We next analyzed the signaling pathways downstream of the insulin receptor to determine which branch of the insulin signaling pathway was responsible for PERK activation in *ob*/*ob* and $Insr^{-/-}$ macrophages. WT mouse macrophages cultured in regular DMEM medium containing 10% FBS were treated with different inhibitors, and P-PERK expression was examined by Western analysis. Interestingly, inhibition of macrophage MEK/ERK activity by PD98059 resulted in a robust induction of P-PERK, similar to ER stress inducers thapsigargin or tunicamycin, whereas treatment with phosphatidylinositol 3-kinase (PI3K), mammalian target of rapamycin, or protein kinase C inhibitors did not result in comparable phosphorylation of PERK (Fig. 2*A*). In addition, because *ob*/*ob* mice have elevated plasma free fatty acid levels, we treated macrophages with palmitate/BSA complexes but did not find any significant induction of P-PERK (Fig. 2*A*). The induction of P-PERK by MEK inhibition was dose dependent and could be triggered by different classes of MEK inhibitors (Fig. 2*B*). In addition, various UPR target genes representing involvement of all three branches of the UPR were induced after MEK inhibition in WT macrophages (Supplementary Fig. 2*A*), resembling the response in $Insr^{-/-}$ and *ob*/*ob* cells (Fig. 1 and Supplementary Fig. 1*C*).

To determine whether MEK inhibitor studies were relevant to the defects associated with insulin-resistant macrophages, we next examined the role of MEK/ERK signaling in apoptotic responses of $Insr^{-/-}$ macrophages. MEK activity, as indicated by the levels of P-ERK, was markedly reduced in Insr-deficient macrophages with or without free cholesterol loading, concomitant with decreased signaling of PI3K and AKT (Fig. 2*C*). To study the contribution of MEK defects to macrophage apoptosis during ER stress, WT cells pretreated with different inhibitors were incubated with free cholesterol or 7-ketocholesterol, and annexin V apoptosis assays were performed. Inhibition of macrophage MEK activity significantly promoted free cholesterol– or 7-ketocholesterol–induced apoptosis compared with untreated controls (Fig. 2*D*), indicating enhanced sensitivity of MEK-defective macrophages to ER stress–associated apoptotic death. Conversely, adenoviral expression of constitutively active MEK in insulin-resistant macrophages (Fig. 2*E*) reduced the levels of P-PERK compared with cells transduced with control lacZ adenovirus (Fig. 2*F*) and significantly rescued these mutant cells from free cholesterol–triggered cell death (Fig. 2*G*), indicating a major role of defective MEK signaling in enhanced apoptosis of insulin-resistant macrophages.

The calcium pump SERCA plays an important role in maintaining ER calcium stores, which are required for proper protein folding (24). Accumulation of free cholesterol in ER membranes was previously shown to inhibit SERCA2b activity and deplete ER calcium stores (25), thereby contributing to free cholesterol–associated apoptosis. In addition, insulin receptor substrate 1 deficiency in mouse pancreatic islets is accompanied by reduced

SERCA2b expression and altered glucose-stimulated calcium signaling (26). Therefore, we next sought to determine whether SERCA2b activity is decreased in insulin-resistant macrophages. Similar to the findings in insulin receptor substrate 1–deficient islets, SERCA2b mRNA and proteins were significantly reduced in *ob/ob* and *Insr*$^{-/-}$ macrophages (Fig. 3*A*). The decrease in SERCA expression was accompanied by depletion of ER calcium pools in *Insr*$^{-/-}$ (Fig. 3*B*) and *ob/ob* (data not shown) macrophages, as indicated by the measurement of releasable ER-stored calcium (9). Moreover, inhibition of MEK activity in WT macrophages led to a significant decrease in Fluo3 fluorescence ratio (Fig. 3*B*), indicating depletion of ER calcium by decreased MEK signaling. Expression of constitutively active MEK in insulin-resistant macrophages induced SERCA mRNA expression (Fig. 3*C*) and subsequently replenished ER calcium stores (Fig. 3*D*). These results suggest a direct role of defective MEK/SERCA activity in increased ER stress–associated apoptosis in insulin-resistant macrophages (Figs. 2 and 3).

Altered SERCA mRNA parallels reduced CREBP activity in insulin-resistant macrophages. The transcription factor CREBP has been reported to support the transcription of SERCA (27,28). To determine whether decreased mRNA expression of SERCA is related to CREBP in insulin-resistant macrophages, we examined the levels of phosphorylation of CREBP at Ser-133 by Western analysis. As shown in Fig. 4*A*, nuclear-phosphorylated CREBP was profoundly reduced in *Insr*$^{-/-}$ macrophages. Accordingly, mRNA levels of known CREBP target genes *c-fos* and *cyclin D* were decreased in MEK-inhibited WT and in *Insr*$^{-/-}$ and *ob/ob* macrophages (data not shown). MEK inhibition by U0126 and PD98059 compounds in WT macrophages led to downregulation of CREBP phosphorylation

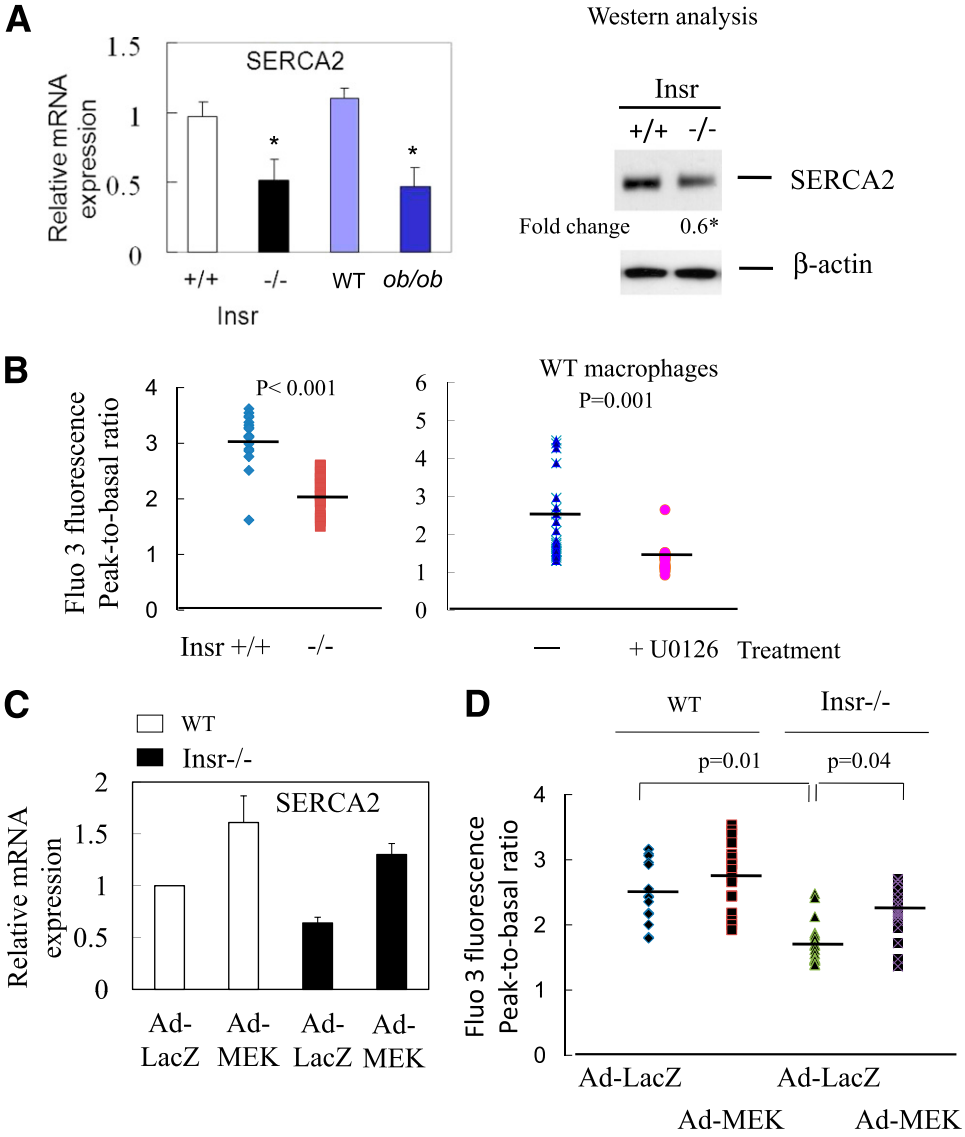

FIG. 3. Reduced MEK signaling in insulin-resistant macrophages results in a decrease in SERCA expression and depletion of ER calcium stores. *A*: The levels of SERCA mRNA and protein in freshly isolated macrophages from *Insr*$^{+/+}$, *Insr*$^{-/-}$, lean WT, and *ob/ob* mice was determined by real-time QPCR and Western analysis. Fold change indicates the expression ratio of *Insr*$^{-/-}$ over *Insr*$^{+/+}$. $n = 4$. *$P < 0.05$ for insulin-resistant macrophages vs. respective control cells. *B*: Releasable ER calcium in individual *Insr*$^{+/+}$ or *Insr*$^{-/-}$ macrophage or WT macrophage pretreated with or without U0126 (5 μmol/L) was measured with calcium indicator Fura3. Fluorescence emission was collected and peak-to-basal fluorescence excitation ratio in individual cells of different groups was shown. $n = 3$. *C*: SERCA mRNA expression in WT or *Insr*$^{-/-}$ macrophages infected with either Ad-LacZ or Ad-MEK as described in Fig. 2*E* was determined by real-time QPCR. $n = 3$. *D*: ER calcium contents in WT or *Insr*$^{-/-}$ macrophages infected with Ad-LacZ or Ad-MEK were measured as described in *B*. $n = 3$. (A high-quality color representation of this figure is available in the online issue.)

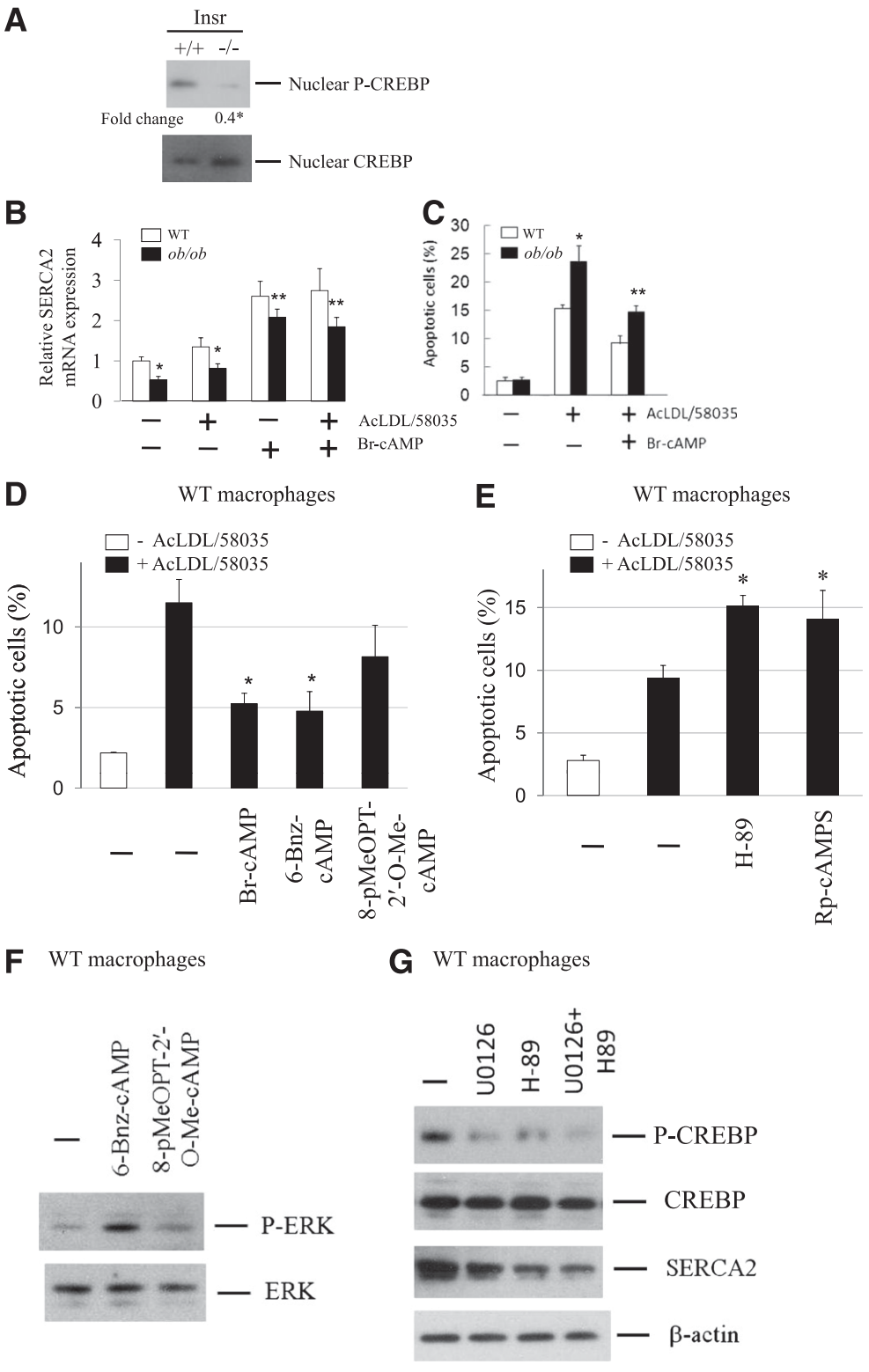

FIG. 4. The activity of transcription factor CREBP downstream of MEK signaling is markedly reduced in insulin-resistant macrophages. *A*: Fresh peritoneal macrophages from either *Insr*$^{+/+}$ or *Insr*$^{-/-}$ mice fed regular chow diet were cultured in DMEM with 10% FBS for 2 h. Cells were harvested and nuclei were fractionated. Nuclear P-CREBP and CREBP were determined by Western analysis with antibodies against the proteins as indicated. Fold change indicates the expression ratio of *Insr*$^{-/-}$ over *Insr*$^{+/+}$. $n = 3$. *$P < 0.05$. *B*: WT or *ob/ob* macrophages were treated with AcLDL (100 μg/mL) and compound 58035 (10 μg/mL) with or without PKA activator Br-cAMP (10 μmol/L) for 8 h. Total RNA was then isolated for real-time QPCR analysis of SERCA2 mRNA expression. QPCR was performed in triplicate. $n = 3$. Averages of two independent experiments were shown. *$P < 0.05$ for WT vs. *ob/ob* cells with or without cholesterol loading. **$P < 0.05$ for *ob/ob* cells with vs. without Br-cAMP treatment. *C*: WT or *ob/ob* macrophages were treated as described in *B*. Apoptosis was determined by annexin V staining. $n = 3$. *$P < 0.05$ for free cholesterol–loaded WT vs. *ob/ob* cells. **$P < 0.05$ for free cholesterol–loaded *ob/ob* cells with vs. without Br-cAMP treatment. *D*: WT macrophages pretreated with or without Br-cAMP (200 μmol/L), 6-Bnz-cAMP (200 μmol/L), or 8-pMeOPT-2′-*O*-MecAMP (200 μmol/L) were incubated with AcLDL and compound 58035. Apoptosis was determined by annexin V staining. *$P < 0.05$ for free cholesterol–loaded cells with vs. without the treatment of cAMP analogs. $n = 3$. *E*: WT macrophages were incubated with AcLDL and compound 58035 with or without PKA inhibitors H-89 (5 μmol/L) or Rp-cAMPS

(see below). Moreover, chromatin immunoprecipitation assays indicated less P-CREBP binding to the SERCA2 promoter in $Insr^{-/-}$ than in control macrophages (Supplementary Fig. 2*B*). In addition, inhibition of macrophage MEK activity resulted in a reduction in P-CREBP binding (Supplementary Fig. 2*C*). Our results suggest that reduced MEK/ERK/nuclear CREBP activity might be responsible for decreased mRNA expression of SERCA and increased ER stress, and contribute to increased apoptosis in insulin-resistant macrophages. To examine whether activation of macrophage CREBP via protein kinase A (PKA) could increase CREBP activity and rescue MEK-defective cells from free cholesterol–induced apoptosis, insulin-resistant *ob*/*ob* cells were incubated with free cholesterol with or without PKA activator 8-bromo-cyclic AMP (Br-cAMP). Br-cAMP stimulated SERCA2b mRNA expression and significantly reduced apoptosis induced by free cholesterol loading in *ob*/*ob* macrophages (Fig. 4*B* and *C*) and $Insr^{-/-}$ cells (data not shown). Adenylyl cyclase activator forskolin exerted a similar effect on apoptosis in these macrophages (data not shown). To further explore whether, in addition to PKA, PKA-independent cAMP effector Epac (exchange nucleotide protein directly activated by cAMP) is involved in cAMP-mediated macrophage protection, we used different cAMP analogs 6-Bnz-cAMP (a PKA activator but poor Epac agonist) and 8-pMeOPT-2'-*O*-Me-cAMP (an Epac activator but poor PKA agonist) to examine the role of Epac signaling in cAMP action. Both 6-Bnz-cAMP and Br-cAMP significantly protected macrophages from free cholesterol–induced apoptosis, whereas the reduction of apoptosis by Epac agonist 8-pMeOPT-2'-*O*-Me-cAMP was less significant compared with PKA activators (Fig. 4*D*).

We next studied the response to ER stress–induced apoptosis of PKA inactivation in macrophages using specific PKA inhibitors H-89 or Rp-cAMPS. Inhibition of macrophage PKA led to an increase in apoptosis of free cholesterol–loaded macrophages (Fig. 4*E*), suggesting an antiapoptotic role of PKA during ER stress. Cyclic AMP and PKA were recently shown to enhance ERK signaling via AKAP-Lbc-KSR-1 (29). In macrophages, PKA activator 6-Bnz-cAMP, but not Epac agonist 8-pMeOPT-2′-*O*-Me-cAMP, stimulated phosphorylation of ERK (Fig. 4*F*). More importantly, specific PKA inhibitor H-89, like MEK inhibitor U0126, decreased the expression of both P-CREBP and SERCA2b in macrophages (Fig. 4*G*). Our results thus indicated that reduced expression of SERCA2b as a result of defective ERK and PKA signaling led to a significant increase in apoptosis in macrophages loaded with free cholesterol (Fig. 2*D* and Fig. 4*E*–*G*).

Exenatide alleviates macrophage ER stress responses and apoptosis in vitro and in vivo. The antidiabetic drug exenatide (exendin 4) increases GLP-1 receptor signaling and has been shown to promote survival of pancreatic β-cells during ER stress (30). Exenatide or GLP-1 treatment leads to activation of PKA, PI3K/AKT, and possibly ERK in these cells (31,32). To investigate whether GLP-1 signaling could rescue insulin-resistant macrophages from ER stress–induced apoptotic death, we examined the responses of primary macrophages to exenatide treatment in vitro. The GLP-1 receptor was readily detected in mouse macrophages, similar to that found in MIN6 mouse pancreatic β-cells, by Western analysis (Supplementary Fig. 3*A*) and was expressed similarly in control and insulin-resistant macrophages (Fig. 5*A*). Both 5′ and 3′ termini of GLP-1 receptor mRNA transcripts could be found in these cells by RT-PCR (data not shown). Protein expression of macrophage GLP-1 receptor could be reduced specifically by small interfering RNA–induced GLP-1 receptor mRNA knockdown (Supplementary Fig. 3*B*). Treatment with GLP-1 receptor agonist exenatide–induced macrophage AKT and ERK phosphorylation (Fig. 5*B*). Moreover, inactivation of macrophage PKA activity by its inhibitor H-89 abolished the increase of ERK phosphorylation by exenatide (Fig. 5*C*), suggesting an involvement of PKA in ERK stimulation. H-89 exerted a similar effect on P-ERK expression in forskolin-treated macrophages (data not shown). Importantly, exenatide significantly increased SERCA2 expression and reduced free cholesterol–induced P-PERK, CHOP, and GADD34 expression and apoptotic death in $Insr^{-/-}$ and WT macrophages (Fig. 5*D*–*F*). A time-course study showed that the decrease in CHOP mRNA expression could be detected as early as 6 h after free cholesterol loading (Supplementary Fig. 3*C*). Exenatide treatment led to a similar significant reduction in apoptosis triggered by free cholesterol or oxysterol in *ob*/*ob* macrophages (Fig. 5*G* and *H*). It is noteworthy that exenatide treatment almost completely reversed the increase in apoptosis associated with cellular insulin resistance in either $Insr^{-/-}$ or *ob*/*ob* macrophages (Fig. 5*F* and *G*), in association with improvements in both ERK and AKT signaling (Fig. 5*B*). Conversely, treatment of insulin-resistant macrophages with PKA inhibitor H-89, thereby decreasing the expression of P-ERK and SERCA2b (Fig. 4*G* and Fig. 5*C*), abolished the exenatide-mediated beneficial effect on cell survival (Fig. 5*I*). Similar results were obtained in cells incubated with another PKA inhibitor, Rp-cAMPS (data not shown).

To examine whether administration of exenatide ameliorates the UPR and apoptosis in macrophages in mouse models of insulin resistance and type 2 diabetes, we used WTD-fed *ob*/*ob*;$Ldlr^{-/-}$ or control $Ldlr^{-/-}$ mice. After 3 months on WTD, mice were injected intraperitoneally daily with either PBS (saline) or exenatide (20 ng/g body weight) for 2 weeks. GLP-1 receptor agonists, including exenatide, are known to reduce food intake and body weight and improve hyperglycemia, peripheral insulin sensitivity, and plasma lipid profiles in mouse models of type 2 diabetes or WTD-fed WT mice (33,34). We also showed that, despite pair feeding and similar changes in body weight, exenatide reduced VLDL/LDL in *ob*/*ob*;$Ldlr^{-/-}$ mice (35). In an attempt to avoid the potentially confounding effects of altered body weight and plasma lipid levels by exenatide, we pair-fed the two groups of mice of the respective genotype during the period of treatment. Exenatide-treated *ob*/*ob* mice had similar body weight and plasma lipid profiles to saline controls after 2 weeks of treatment (Supplementary Fig. 4*A* and *B*). Systemic insulin sensitivity was also not significantly changed by exenatide treatment, as assessed by intraperitoneal glucose tolerance test (Supplementary Fig. 4*C*). A similar response was also found in exenatide- versus PBS-treated $Ldlr^{-/-}$ mice (data not shown). To determine whether macrophage UPR was reduced in vivo by

(100 μmol/L). Apoptosis was determined by annexin V staining. *$P < 0.05$ for free cholesterol–loaded cells with vs. without the treatment of inhibitors. $n = 3$. *F*: WT macrophages were treated with or without 6-Bnz-cAMP (200 μmol/L) or 8-pMeOPT-2'-*O*-Me-cAMP (200 μmol/L) for 20 min. The levels of P-ERK and total ERK were determined by Western analysis. $n = 3$. *G*: WT macrophages were treated with or without U0126 (10 μmol/L) or H-89 (5 μmol/L) or in combination for 5 h. The levels of indicated proteins were determined by Western analysis. $n = 3$.

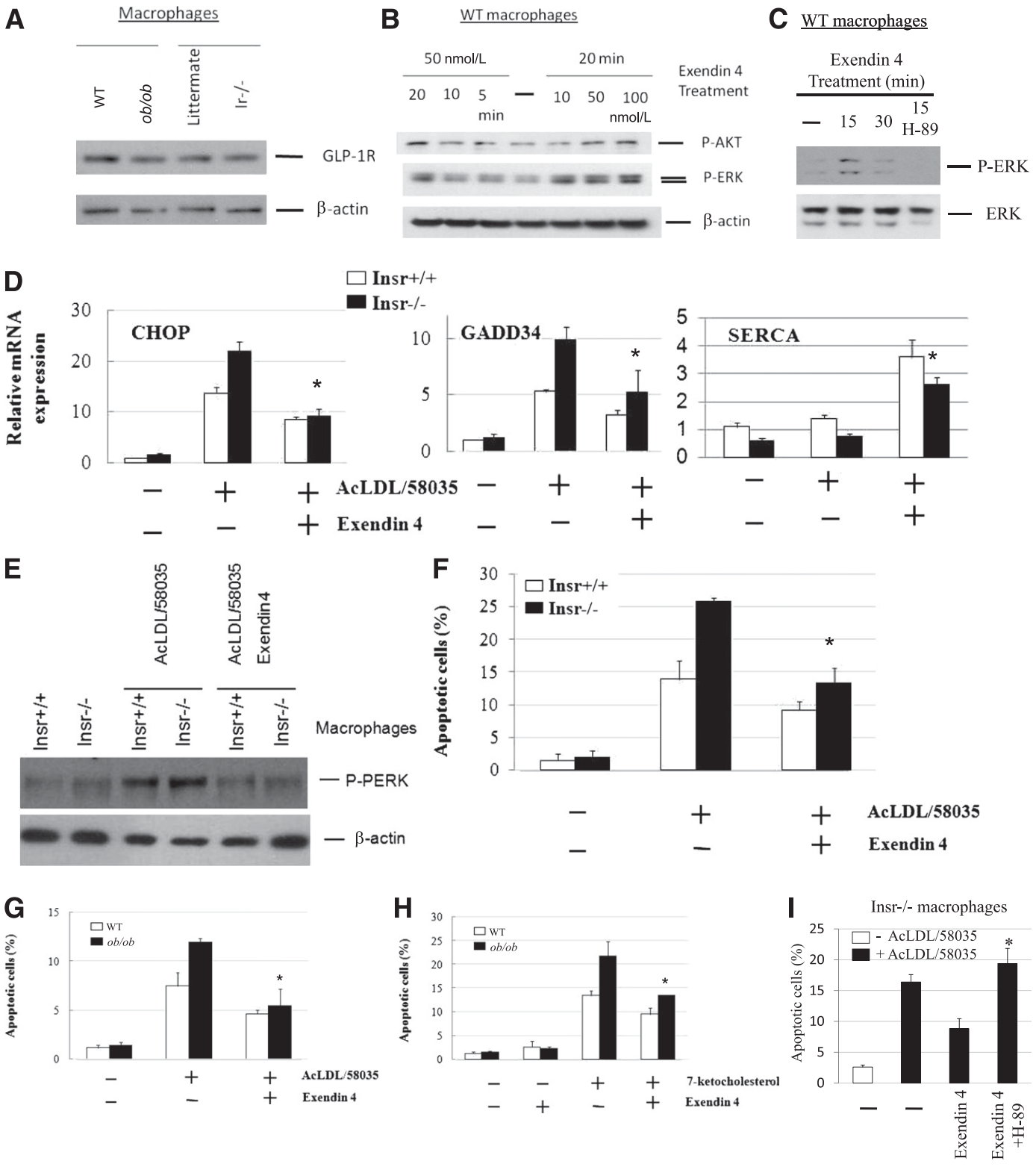

FIG. 5. GLP-1 receptor agonist exenatide ex vivo protects insulin-resistant macrophages from ER stress–induced apoptosis. *A*: The levels of GLP-1 receptor in primary macrophages from lean WT, *ob/ob*, *Insr*$^{+/+}$, and *Insr*$^{-/-}$ mice were determined by Western analysis. $n = 3$. *B*: Temporal and dose responses to GLP-1 receptor agonist exenatide (exendin-4) of AKT and ERK phosphorylation in WT macrophages were determined by Western analysis. $n = 3$. *C*: WT macrophages were incubated with exendin 4 (100 nmol/L) with or without pretreatment of PKA inhibitor H-89 (5 μmol/L) for indicated times. The expression of P-ERK and ERK was measured by Western analysis. $n = 3$. *D*: Primary *Insr*$^{+/+}$ or *Insr*$^{-/-}$ macrophages were incubated with AcLDL (100 μg/mL) and compound 58035 (10 μg/mL) with or without exendin-4 (100 nmol/L) for 8 h. CHOP, GADD34, and SERCA mRNA expression was measured by real-time QPCR analysis. $n = 3$. *$P < 0.05$ for free cholesterol–loaded cells with vs. without the treatment of exendin-4. *E*: Primary macrophages treated as described in *D* were used for determination of P-PERK expression by Western analysis. $n = 3$. *F*: Primary *Insr*$^{+/+}$ and *Insr*$^{-/-}$ macrophages treated for 8 h as similarly described in *D* were assayed for apoptosis by annexin V staining. *$P < 0.05$ for free cholesterol–loaded cells with vs. without the treatment of exendin-4. $n = 3$. *G* and *H*: WT and *ob/ob* macrophages were treated with or without exendin-4 (100 nmol/L) followed by incubation with or without AcLDL (100 μg/mL) and compound 58035 (10 μg/mL) or 7-ketocholesterol (40 μg/mL) for 8 h. Apoptosis of macrophages was determined by annexin V staining. $n = 3$. *$P < 0.05$ for free cholesterol– or oxysterol-loaded cells with

exenatide, we harvested peritoneal macrophages after treatment. In the basal state, primary *ob/ob* macrophages from exenatide-treated mice showed a significant elevation of SERCA levels and normalization of ER calcium stores accompanied by a significant reduction in expression of UPR markers P-PERK, CHOP, spliced Xbp1, and 78-kDa glucose-regulated protein (immunoglobulin-binding protein) (Fig. 6*A* and Supplementary Fig. 4*D* and *E*), indicating in vivo exenatide-mediated attenuation of macrophage UPR independent of plasma lipid parameters or systemic insulin sensitivity. Moreover, these cells from exenatide-treated mice were significantly less susceptible to apoptosis induced by free cholesterol or 7-ketocholesterol (Fig. 6*B*).

Next, we investigated in vivo effects of exenatide treatment compared with saline on macrophage UPR and apoptosis in atherosclerotic lesions in *ob/ob.Ldlr*$^{-/-}$ versus *Ldlr*$^{-/-}$ mice. ATF-3 and P-PERK, among other UPR markers, were previously used in atherosclerosis studies. Like P-PERK, ATF-3 is induced by MEK inhibitors in peritoneal macrophages (Supplementary Fig. 4*E*). Its expression is increased in *ob/ob* versus WT macrophages and is normalized in vivo by exenatide (Supplementary Fig. 4*E*). Double immunofluorescence with antibodies against ATF-3 or P-PERK and against macrophage marker Mac-3 was carried out. As shown in Supplementary Fig. 4*F* and *G*, ATF-3 and P-PERK staining is increased in atherosclerotic lesions of *ob/ob.Ldlr*$^{-/-}$ compared with *Ldlr*$^{-/-}$ mice treated with saline. ATF-3–positive lesional macrophages in *ob/ob.Ldlr*$^{-/-}$ mice were significantly reduced in percentage by exenatide treatment (Fig. 6*C*). A similar response to exenatide of macrophage P-PERK in the lesions of obese mice was also found (Fig. 6*C*). Macrophage apoptosis in atherosclerotic plaques was evaluated by active caspase-3 expression and TUNEL assay (15). In vivo exenatide significantly attenuated lesional macrophage apoptosis in *ob/ob.Ldlr*$^{-/-}$, but not in *Ldlr*$^{-/-}$, mice (Fig. 6*D*). Both macrophage ATF-3 and caspase-3 expression in the lesions of *Insr*$^{-/-}$*.Ldlr*$^{-/-}$ mice was also reduced by exenatide (Supplementary Fig. 4*H*). Preliminary results revealed that exenatide during short periods of treatment did not significantly alter the sizes of atherosclerotic lesions and necrotic cores in *ob/ob.Ldlr*$^{-/-}$ and *Ldlr*$^{-/-}$ mice (data not shown).

DISCUSSION

Defective insulin signaling in macrophage foam cells promotes ER stress–associated apoptotic death in atherosclerotic lesions (15,16). In the current study, we show defects of macrophage MEK signaling and SERCA activity as a key mechanism underlying the impaired survival of stressed macrophage foam cells. Perturbation of calcium homeostasis in insulin-resistant cells as a result of reduced SERCA activity and subsequent release of ER calcium stores triggers the UPR and increases susceptibility to apoptotic death in response to "second hits" with additional adverse stimuli, such as overload with free cholesterol, oxidized lipids such as 7-oxysterols, oxidized phospholipids present in oxidized LDL, or apoptotic cells (Fig. 7).

The ER stress response is associated with transient activation of both MEK/ERK and AKT signaling pathways, and both have antiapoptotic activity in this context (36). Macrophage and vascular AKT have been shown to be protective of lesional apoptosis and the development of atherosclerosis (15,37). Our previous studies showed decreased AKT and increased nuclear FoxO1 in insulin-resistant macrophages during the ER stress response, resulting in induction of IkBε and an attenuated nuclear factor-κB/p65 response with proapoptotic and anti-inflammatory consequences during the ER stress response (20) (Fig. 7). However, increased macrophage FoxO1 activity only led to increased apoptosis in the presence of an ER stressor, such as free cholesterol loading or thapsigargin, and active FoxOs1/3 did not induce ER stress per se (20). Thus, decreased AKT/increased FoxO1 could not explain the enhanced ER stress response seen in insulin-resistant cells (Figs. 1 and 2 and Supplementary Fig. 1). The current study shows that decreased MEK/ERK signaling is primarily responsible for more prominent activation of the UPR in insulin-resistant macrophages. MEK signaling is involved in the regulation of various cellular activities, including apoptosis. During ER stress induced by thapsigargin, tunicamycin, or free cholesterol, MEK/ERK signaling is transiently activated (16). Inhibition of MEK activity has been shown to increase apoptosis in a variety of cell lines in response to ER stress (38,39), but the relevant mechanisms have not been well defined. Our findings indicate a link between macrophage MEK signaling and ER-resident SERCA activity. Attenuation of the MEK/ERK signaling cascade and subsequent reduction of SERCA activity and depletion of ER calcium stores sensitized insulin-resistant cells to ER stress–associated apoptotic stimuli more than normal controls (Figs. 2 and 3). Expression of constitutively active MEK rescued the defect in SERCA and P-PERK expression and partly decreased the enhanced apoptotic response of insulin-resistant cells. The fact that rescue of apoptosis was incomplete was expected since reconstitution of MEK/ERK activity did not restore defective AKT signaling in these cells. In contrast, treatment with agents that increased cellular cAMP, such as exenatide and forskolin, restored both ERK and AKT signaling pathways in insulin-resistant macrophages, and reversed their increased susceptibility to apoptotic death during free cholesterol or oxysterol loading (Figs. 4–6).

Our results indicate that macrophage insulin resistance promotes ER stress–associated apoptotic death partly through defects in SERCA and calcium mobilization. The calcium pump SERCA plays a major role in the regulation of cellular calcium homeostasis. The generation of a concentration gradient of calcium across the ER membrane requires SERCA activity. ER luminal calcium is essential for proper processing, folding, and maturation of proteins in the ER (24). Perturbation of the ER calcium flux as a result of decreased SERCA activity, such as in insulin-resistant macrophages, activates the UPR. The increase in cytosolic calcium caused by decreased SERCA might also be expected to directly promote the apoptotic response (21,40). A reduction in SERCA activity, rather than an increase in the activity of ER-resident inositol trisphosphate receptors and ryanodine receptors, was shown to trigger major ER stress–associated apoptosis in cultured β-cells (41,42). Consistent with our findings in

vs. without the treatment of exendin-4. *I*: *Insr*$^{-/-}$ macrophages were treated with or without exendin-4 (100 nmol/L) or exendin-4 plus PKA inhibitor H-89 (5 μmol/L) followed by incubation with or without AcLDL and compound 58035. Apoptosis of macrophages was determined by annexin V staining. *$P < 0.05$ for free cholesterol–loaded cells with exendin-4 vs. exendin-4 + H-89 treatment. $n = 3$.

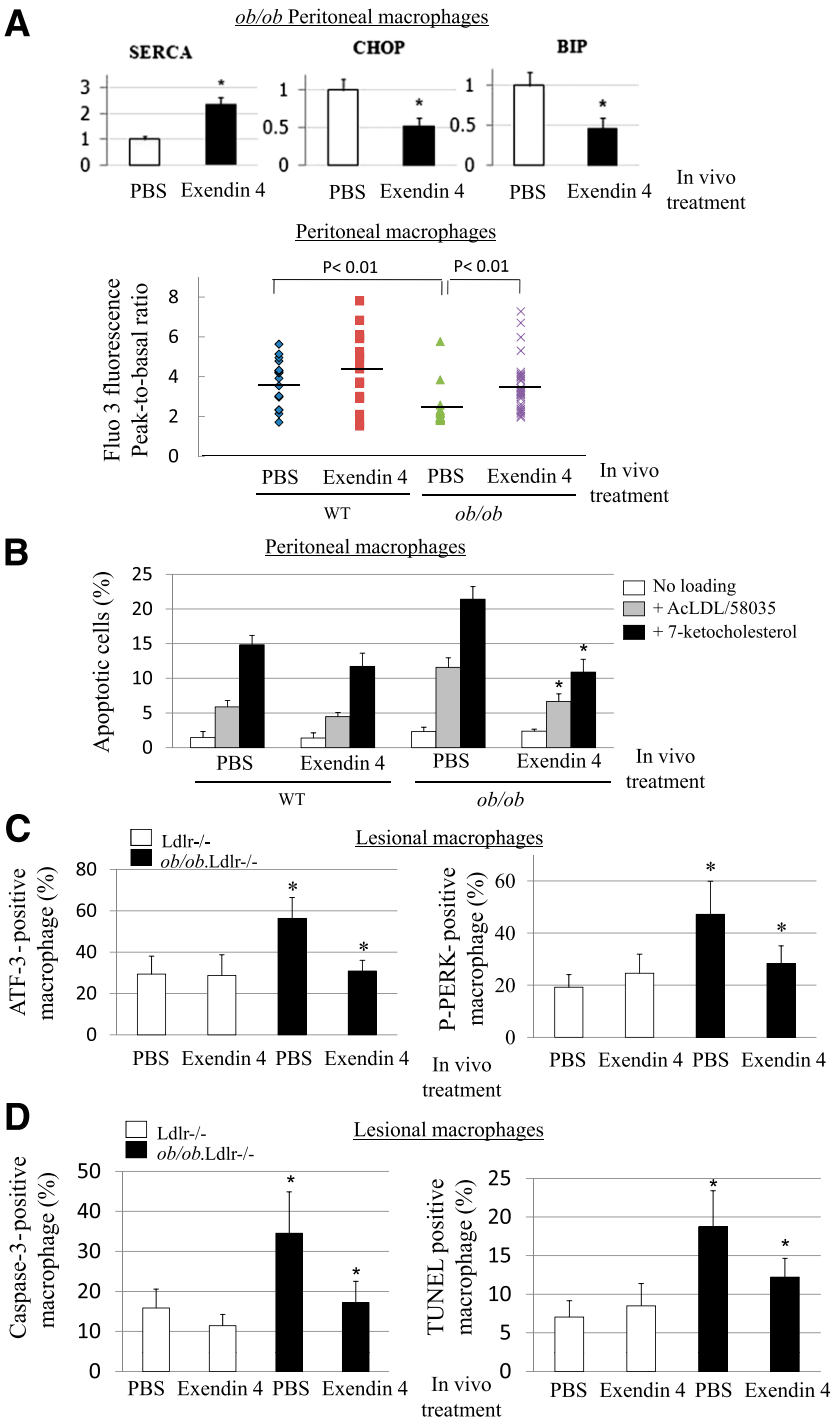

FIG. 6. GLP-1 receptor agonist exenatide in vivo reduces basal UPR and apoptosis in macrophages of *ob/ob;Ldlr*$^{-/-}$ mice independent of plasma lipid profiles or systemic insulin sensitivity. *A*, *top*: Primary macrophages were isolated from *ob/ob;Ldlr*$^{-/-}$ mice fed WTD for 3 months and then administered either PBS or exendin 4 (20 ng/g body weight) for 2 weeks under pair-feeding condition (n = 4 for each group), and total RNA was then isolated for real-time QPCR analysis of SERCA2, CHOP, and immunoglobulin-binding protein (BIP) mRNA expression. *P < 0.05 for primary macrophages with vs. without in vivo treatment of exendin-4. *A*, *bottom*: Releasable ER calcium in individual primary macrophages isolated from WT or *ob/ob* mice pretreated in vivo with PBS or exendin 4 was measured with calcium indicator Fura3. Fluorescence emission was collected, and peak-to-basal fluorescence excitation ratio in individual cells of different groups was shown. n = 3. *B*: Primary macrophages from WTD-fed WT or *ob/ob* mice receiving either PBS or exendin-4 in vivo were treated with or without AcLDL (100 μg/mL) and compound 58035 (10 μg/mL) or 7-ketocholesterol (40 μg/mL). Apoptosis of macrophages was determined by annexin V staining. *P < 0.05 for free cholesterol– or oxysterol-loaded cells with PBS vs. exendin-4 treatment. n = 3. *C*: Double immunofluorescence staining using antibodies against UPR markers ATF-3 or P-PERK and macrophage marker Mac-3 in atherosclerotic lesions of *ob/ob.Ldlr*$^{-/-}$ and *Ldlr*$^{-/-}$ mice with in vivo treatment of PBS or exendin-4. The data of ATF-3– or P-PERK–positive macrophages are expressed as percentage of total macrophages in the same lesion areas. *P < 0.05 for saline-treated *ob/ob.Ldlr*$^{-/-}$ vs. saline-treated *Ldlr*$^{-/-}$ or vs. exendin-4–treated *ob/ob.Ldlr*$^{-/-}$ mice. n = 4–6. *D*: Apoptotic macrophages in atherosclerotic plaques of *ob/ob.Ldlr*$^{-/-}$ and *Ldlr*$^{-/-}$ mice with in vivo treatment of PBS or exendin-4 were detected by active caspase-3 or TUNEL as well as Mac-3 costaining. The data of caspase-3– or TUNEL-positive macrophages are expressed as percentage of total macrophages in the same lesion areas. *P < 0.05 for saline-treated *ob/ob.Ldlr*$^{-/-}$ vs. saline-treated *Ldlr*$^{-/-}$ or vs. exendin-4–treated *ob/ob.Ldlr*$^{-/-}$ mice. n = 4–6. (A high-quality color representation of this figure is available in the online issue.)

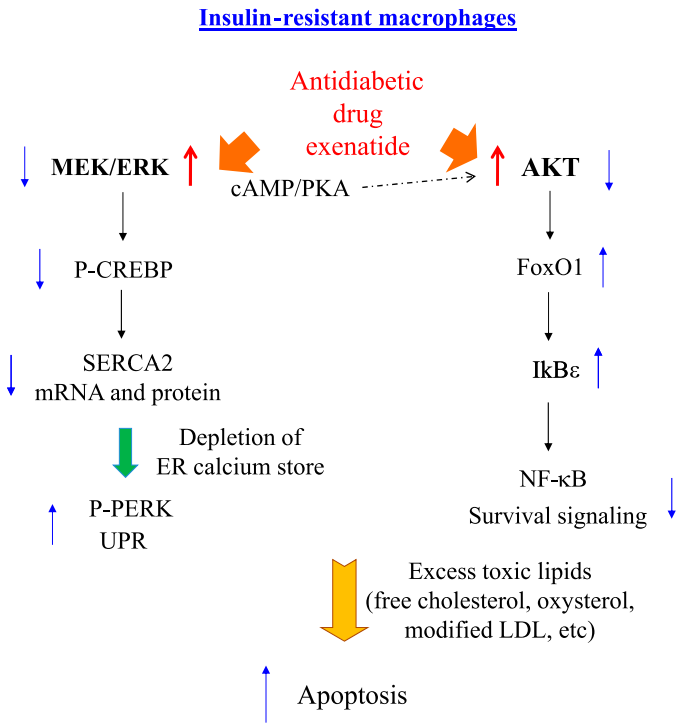

FIG. 7. A schematic representation of the mechanisms of increased macrophage apoptosis in insulin-resistant states and reversal by the antidiabetic drug exenatide. Cellular insulin resistance in cells of the arterial wall, including macrophages, promotes moderate ER stress responses and predisposes to apoptosis in the lesion environment. Defective MEK signaling and decreased SERCA activity in insulin-resistant macrophages cause depletion of ER calcium stores and evoke the UPR. Under sustained stress conditions such as free cholesterol or oxysterol overload, these cells exhibit attenuated responses of AKT and MEK with more robust induction of apoptosis. Increased signaling via GLP-1 receptor by exenatide may offer a way to rescue these macrophages from ER stress responses and apoptosis in atherosclerotic plaques in type 2 diabetes and insulin resistance.

insulin-resistant macrophages, SERCA expression or activity is reduced in the islets, liver, heart, and platelets in type 2 diabetes and insulin resistance (26,43–45), suggesting a perturbed mobilization of intracellular calcium in these tissues. The contribution of impaired SERCA to ER stress and insulin resistance found in *ob/ob* liver (44,45) illustrates an important role of SERCA in the development of metabolic derangements in type 2 diabetes and insulin resistance.

Our in vitro and in vivo findings (summarized in Fig. 7) suggest potential atheroprotective benefits of the antidiabetic drug exenatide in type 2 diabetes. We showed that exenatide alleviates cellular ER stress and reduces apoptotic death in lesional macrophages of mouse models of type 2 diabetes and insulin resistance (Fig. 6 and Supplementary Fig. 4), likely involving the activation of both PKA or MEK/SERCA and AKT prosurvival signaling (Figs. 5 and 6). In stressed pancreatic β-cells treated with the SERCA inhibitor thapsigargin, Drucker and colleagues (30) showed that exenatide ameliorates ER stress–induced apoptosis by magnifying feedback attenuation of P-eIF2α by GADD34-associated phosphatase. In WTD-fed *ob/ob*;*Ldlr*$^{-/-}$ mice, we showed increased SERCA expression/activity and reduced ER stress responses as well as apoptosis of macrophages, without changes in plasma lipids or insulin resistance (Fig. 6). Thus, our findings offer new insights into the mechanisms of protection against apoptotic cell death by exenatide, and suggest that exenatide or similar therapies may offer a way to improve atherosclerosis in insulin resistance and type 2 diabetes by reversing the adverse effects of enhanced apoptosis during lesion development.

ACKNOWLEDGMENTS

This study was supported by National Institutes of Health grants HL-087123 and HL-075662.

No potential conflicts of interest relevant to this article were reported.

C.-P.L. researched and evaluated data and wrote the manuscript. S.H. and G.L. researched data and reviewed the manuscript. I.T. and A.R.T. evaluated data and reviewed and edited the manuscript. C.-P.L. is the guarantor of this work and, as such, had full access to all the data in the study and takes responsibility for the integrity of the data and the accuracy of the data analysis.

The authors thank Dr. Carrie Welch and Sandra Abramowicz (Columbia University) for preparation of paraffin sections of mouse proximal aortas.

REFERENCES

1. Mazzone T, Chait A, Plutzky J. Cardiovascular disease risk in type 2 diabetes mellitus: insights from mechanistic studies. Lancet 2008;371:1800–1809
2. Burke AP, Kolodgie FD, Zieske A, et al. Morphologic findings of coronary atherosclerotic plaques in diabetics: a postmortem study. Arterioscler Thromb Vasc Biol 2004;24:1266–1271
3. Glass CK, Witztum JL. Atherosclerosis. the road ahead. Cell 2001;104:503–516
4. Boullier A, Li Y, Quehenberger O, et al. Minimally oxidized LDL offsets the apoptotic effects of extensively oxidized LDL and free cholesterol in macrophages. Arterioscler Thromb Vasc Biol 2006;26:1169–1176
5. Gargalovic PS, Gharavi NM, Clark MJ, et al. The unfolded protein response is an important regulator of inflammatory genes in endothelial cells. Arterioscler Thromb Vasc Biol 2006;26:2490–2496
6. Rusiñol AE, Thewke D, Liu J, Freeman N, Panini SR, Sinensky MS. AKT/protein kinase B regulation of BCL family members during oxysterol-induced apoptosis. J Biol Chem 2004;279:1392–1399
7. Tabas I. The role of endoplasmic reticulum stress in the progression of atherosclerosis. Circ Res 2010;107:839–850
8. Kharroubi I, Ladrière L, Cardozo AK, Dogusan Z, Cnop M, Eizirik DL. Free fatty acids and cytokines induce pancreatic beta-cell apoptosis by different mechanisms: role of nuclear factor-kappaB and endoplasmic reticulum stress. Endocrinology 2004;145:5087–5096
9. Feng B, Yao PM, Li Y, et al. The endoplasmic reticulum is the site of cholesterol-induced cytotoxicity in macrophages. Nat Cell Biol 2003;5:781–792
10. Pedruzzi E, Guichard C, Ollivier V, et al. NAD(P)H oxidase Nox-4 mediates 7-ketocholesterol-induced endoplasmic reticulum stress and apoptosis in human aortic smooth muscle cells. Mol Cell Biol 2004;24:10703–10717
11. Myoishi M, Hao H, Minamino T, et al. Increased endoplasmic reticulum stress in atherosclerotic plaques associated with acute coronary syndrome. Circulation 2007;116:1226–1233
12. Thorp E, Li G, Seimon TA, Kuriakose G, Ron D, Tabas I. Reduced apoptosis and plaque necrosis in advanced atherosclerotic lesions of Apoe-/- and Ldlr-/- mice lacking CHOP. Cell Metab 2009;9:474–481
13. Erbay E, Babaev VR, Mayers JR, et al. Reducing endoplasmic reticulum stress through a macrophage lipid chaperone alleviates atherosclerosis. Nat Med 2009;15:1383–1391
14. Dong Y, Zhang M, Liang B, et al. Reduction of AMP-activated protein kinase alpha2 increases endoplasmic reticulum stress and atherosclerosis in vivo. Circulation 2010;121:792–803
15. Han S, Liang CP, DeVries-Seimon T, et al. Macrophage insulin receptor deficiency increases ER stress-induced apoptosis and necrotic core formation in advanced atherosclerotic lesions. Cell Metab 2006;3:257–266
16. Liang CP, Han S, Senokuchi T, Tall AR. The macrophage at the crossroads of insulin resistance and atherosclerosis. Circ Res 2007;100:1546–1555
17. Komura T, Sakai Y, Honda M, Takamura T, Matsushima K, Kaneko S. CD14+ monocytes are vulnerable and functionally impaired under endoplasmic reticulum stress in patients with type 2 diabetes. Diabetes 2010;59:634–643

18. Laybutt DR, Preston AM, Akerfeldt MC, et al. Endoplasmic reticulum stress contributes to beta cell apoptosis in type 2 diabetes. Diabetologia 2007;50:752–763
19. Liang CP, Han S, Okamoto H, et al. Increased CD36 protein as a response to defective insulin signaling in macrophages. J Clin Invest 2004;113:764–773
20. Senokuchi T, Liang CP, Seimon TA, et al. Forkhead transcription factors (FoxOs) promote apoptosis of insulin-resistant macrophages during cholesterol-induced endoplasmic reticulum stress. Diabetes 2008;57:2967–2976
21. Li G, Mongillo M, Chin K-T, et al. Role of ERO1-alpha-mediated stimulation of inositol 1,4,5-triphosphate receptor activity in endoplasmic reticulum stress-induced apoptosis. J Cell Biol 2009;186:783–792
22. Seimon TA, Wang Y, Han S, et al. Macrophage deficiency of p38alpha MAPK promotes apoptosis and plaque necrosis in advanced atherosclerotic lesions in mice. J Clin Invest 2009;119:886–898
23. Marciniak SJ, Ron D. Endoplasmic reticulum stress signaling in disease. Physiol Rev 2006;86:1133–1149
24. Brostrom MA, Brostrom CO. Calcium dynamics and endoplasmic reticular function in the regulation of protein synthesis: implications for cell growth and adaptability. Cell Calcium 2003;34:345–363
25. Li Y, Ge M, Ciani L, et al. Enrichment of endoplasmic reticulum with cholesterol inhibits sarcoplasmic-endoplasmic reticulum calcium ATPase-2b activity in parallel with increased order of membrane lipids: implications for depletion of endoplasmic reticulum calcium stores and apoptosis in cholesterol-loaded macrophages. J Biol Chem 2004;279:37030–37039
26. Kulkarni RN, Roper MG, Dahlgren G, et al. Islet secretory defect in insulin receptor substrate 1 null mice is linked with reduced calcium signaling and expression of sarco(endo)plasmic reticulum Ca2+-ATPase (SERCA)-2b and -3. Diabetes 2004;53:1517–1525
27. Moriscot AS, Sayen MR, Hartong R, Wu P, Dillmann WH. Transcription of the rat sarcoplasmic reticulum Ca2+ adenosine triphosphatase gene is increased by 3,5,3′-triiodothyronine receptor isoform-specific interactions with the myocyte-specific enhancer factor-2a. Endocrinology 1997;138:26–32
28. Ulianich L, Secondo A, De Micheli S, et al. TSH/cAMP up-regulate sarco/endoplasmic reticulum Ca2+-ATPases expression and activity in PC Cl3 thyroid cells. Eur J Endocrinol 2004;150:851–861
29. Smith FD, Langeberg LK, Cellurale C, et al. AKAP-Lbc enhances cyclic AMP control of the ERK1/2 cascade. Nat Cell Biol 2010;12:1242–1249
30. Yusta B, Baggio LL, Estall JL, et al. GLP-1 receptor activation improves beta cell function and survival following induction of endoplasmic reticulum stress. Cell Metab 2006;4:391–406
31. Buteau J, Roduit R, Susini S, Prentki M. Glucagon-like peptide-1 promotes DNA synthesis, activates phosphatidylinositol 3-kinase and increases transcription factor pancreatic and duodenal homeobox gene 1 (PDX-1) DNA binding activity in beta (INS-1)-cells. Diabetologia 1999;42:856–864
32. Gomez E, Pritchard C, Herbert TP. cAMP-dependent protein kinase and Ca2+ influx through L-type voltage-gated calcium channels mediate Raf-independent activation of extracellular regulated kinase in response to glucagon-like peptide-1 in pancreatic beta-cells. J Biol Chem 2002;277:48146–48151
33. Ding X, Saxena NK, Lin S, Gupta NA, Anania FA. Exendin-4, a glucagon-like protein-1 (GLP-1) receptor agonist, reverses hepatic steatosis in ob/ob mice. Hepatology 2006;43:173–181
34. Young AA, Gedulin BR, Bhavsar S, et al. Glucose-lowering and insulin-sensitizing actions of exendin-4: studies in obese diabetic (ob/ob, db/db) mice, diabetic fatty Zucker rats, and diabetic Rhesus monkeys (*Macaca mulatta*). Diabetes 1999;48:1026–1034
35. Liang CP, and Tall AR. Exenatide reverses atherogenic dyslipidemia in type 2 diabetes likely by direct suppression of inflammatory macrophage response. Diabetes 2011;60(Suppl. 1), Late Breaking 5-LB
36. Hu P, Han Z, Couvillon AD, Exton JH. Critical role of endogenous Akt/IAPs and MEK1/ERK pathways in counteracting endoplasmic reticulum stress-induced cell death. J Biol Chem 2004;279:49420–49429
37. Fernández-Hernando C, Ackah E, Yu J, et al. Loss of Akt1 leads to severe atherosclerosis and occlusive coronary artery disease. Cell Metab 2007;6:446–457
38. Hung CC, Ichimura T, Stevens JL, Bonventre JV. Protection of renal epithelial cells against oxidative injury by endoplasmic reticulum stress preconditioning is mediated by ERK1/2 activation. J Biol Chem 2003;278:29317–29326
39. Jiang CC, Chen LH, Gillespie S, et al. Inhibition of MEK sensitizes human melanoma cells to endoplasmic reticulum stress-induced apoptosis. Cancer Res 2007;67:9750–9761
40. Timmins JM, Ozcan L, Seimon TA, et al. Calcium/calmodulin-dependent protein kinase II links ER stress with Fas and mitochondrial apoptosis pathways. J Clin Invest 2009;119:2925–2941
41. Cardozo AK, Ortis F, Storling J, et al. Cytokines downregulate the sarcoendoplasmic reticulum pump Ca2+ ATPase 2b and deplete endoplasmic reticulum Ca2+, leading to induction of endoplasmic reticulum stress in pancreatic beta-cells. Diabetes 2005;54:452–461
42. Luciani DS, Gwiazda KS, Yang TL, et al. Roles of IP3R and RyR Ca2+ channels in endoplasmic reticulum stress and beta-cell death. Diabetes 2009;58:422–432
43. Wold LE, Dutta K, Mason MM, et al. Impaired SERCA function contributes to cardiomyocyte dysfunction in insulin resistant rats. J Mol Cell Cardiol 2005;39:297–307
44. Park SW, Zhou Y, Lee J, Lee J, Ozcan U. Sarco(endo)plasmic reticulum Ca2+-ATPase 2b is a major regulator of endoplasmic reticulum stress and glucose homeostasis in obesity. Proc Natl Acad Sci USA 2010;107:19320–19325
45. Fu S, Yang L, Li P, et al. Aberrant lipid metabolism disrupts calcium homeostasis causing liver endoplasmic reticulum stress in obesity. Nature 2011;473:528–531